

Experimental reconstruction of a nonlocal nonlinear response function of a thermal medium

Alexander E. Minovich^a, Kaloyan S. Bezuhanov^b, Dragomir N. Neshev^{*a}, Alexander A. Dreischuh^{ab},
Wieslaw Z. Krolikowski^c, Yuri S. Kivshar^a

^aNonlinear Physics Centre, Research School of Physical Sciences and Engineering,
Australian National University, Canberra ACT 0200, Australia

^bDepartment of Quantum Electronics, Faculty of Physics, Sofia University,
5, J. Bourchier Blvd., BG-1164 Sofia, Bulgaria

^cLaser Physics Centre, Research School of Physical Sciences and Engineering,
Australian National University, Canberra ACT 0200, Australia

ABSTRACT

We present a novel experimental technique for retrieving the spatial profile of a nonlocal response function in a medium with thermal nonlinearity. Our method is based on the quantitative measurement of the light-induced nonlinear phase distribution by holographic interferometry combined with an iterative process of two-dimensional deconvolution using the known pump beam intensity distribution.

Keywords: nonlocality, nonlocal response function, thermal nonlinearity, deconvolution

1. INTRODUCTION

Nonlinear response of the medium to an external action $I(x,y)$ is spatially *nonlocal* when it depends not only on the action in the point (x,y) but also in the neighboring points, $I(x',y')$. Such response can be described by a phenomenological model $\Delta n(x,y) = \iint R(|x-x'|, |y-y'|) I(x',y') dx' dy'$, where $\Delta n(x,y)$ represents, for instance, nonlinear refractive index change of the optical medium and $R(x,y)$ stands for the nonlocal response function. Nonlocality appears naturally in many physical processes such as plasma heating and ionization¹, optical pumping of atoms², drift and/or diffusion of photo-excited carriers in photorefractive media³⁻⁴, etc. Similarly, the heat conduction in materials with thermal nonlinearity results in a spatially nonlocal change in the refractive index⁵⁻⁷. While in most of the studies the spatial nonlocality is considered to be symmetric, the symmetry can be broken by asymmetric boundary conditions⁷. It is worth to mention that nonlocality may also exist in temporal domain. There it describes a non-instantaneous response of the medium, and it is often an asymmetric function of time because of causality constrains, as in the case of the Raman effect in optical pulses⁸ or lidar return due to arbitrary-shaped laser pulses⁹. Recent studies of nonlinear effects in nonlocal nonlinear media include the exact analytical solutions for one-dimensional bright and dark solitons for weak nonlocality¹⁰, prediction of existence of stable ring vortex solitons in self-focusing media in the regime of strong nonlocality^{11,12}, as well as demonstration of a dramatic effect of nonlocality on both interaction forces between dark spatial solitons¹³ and soliton mobility in optical lattices¹⁴. Because of a crucial importance of nonlocal nonlinear phenomena, the quantitative characterization of nonlocality of the nonlinear optical response is of a great practical interest.

2. PHENOMENOLOGICAL MODEL AND THE ASSOCIATED INVERSE PROBLEM

In this analysis we adopt the phenomenological model of a Kerr-type nonlinear optical medium, in which the refractive index $n = n_0 + \Delta n(I(x,y,z))$ is a spatially nonlocal function of the light intensity $I(x,y,z)$

$$\Delta n(I(x,y)) = \Delta n_0 \iint R(x-x', y-y') I(x',y') dx' dy' / \iint R(x-x', y-y') dx' dy' , \quad (1)$$

where Δn_0 is the maximal refractive index change accessible in the local case and the integration spans over all space. The width of the response function $R(x,y)$ relative to the width of the intensity profile determines the degree of the

*dnn124@rsphysse.anu.edu.au; phone +61-2-6125-3792; fax +61-2-6125-8588; <http://www.rsphysse.anu.edu.au/nonlinear/>

nonlocality¹⁵. The evolution of optical beams in media described by the nonlocal model Eq. 1 is governed by the so called nonlocal Schrödinger equation. While, in general this equation has to be solved numerically, few limiting cases allow for an analytical treatment. In particular, in a highly-nonlocal limit the beam evolution is described by the equation of a linear harmonic oscillator¹⁶. Also, the logarithmic model of nonlinearity leads to an exact analytical treatment¹⁷. Finally, for the case of weak nonlocality the corresponding modified nonlinear Schrödinger equation admits exact, bright and dark, one-dimensional soliton solutions¹⁰. Although Eq. 1 is just a phenomenological model it nevertheless adequately describes many real physical situations¹⁰. Therefore the knowledge of the actual form of the response functions of the nonlinear media is important in evaluating of the possible impact of the nonlocality on beam evolution. In Fig.1 we illustrate the extreme (but physical) situation of a highly elliptical laser beam propagating in a medium with a strong anisotropic nonlocality. Assuming elliptic Gaussian profiles of both $I(x,y)$ and $R(x,y)$ (e.g. $I(x',y')=\exp\{-(x'/a)^2-(y'/b)^2\}$ and $R(x-x',y-y')=\exp\{-(x-x')^2/c^2-(y-y')^2/d^2\}$), the effective refractive index change can appear nearly axially symmetric provided the nonlocality is strongest in the direction, in which the optical beam is narrow. This effect is intuitively clear since the nonlocality acts to smooth out and broaden the refractive index profile induced by the finite beams.

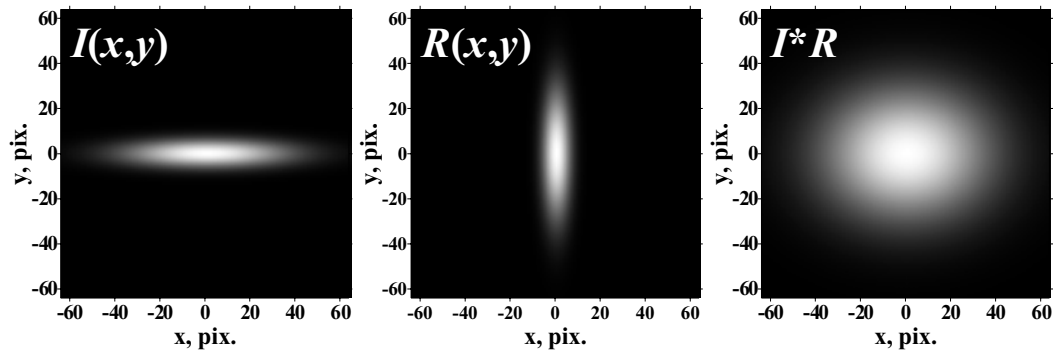


Fig. 1. Intensity distribution $I(x,y)$, nonlocal response function $R(x,y)$ and refractive index change $\Delta n(I(x,y))/\Delta n_0=I^*R$ showing improved symmetry due to the anisotropic nonlocality. [$I(x,y)=\exp\{-(x/a)^2-(y/b)^2\}$, $a^2=36$, $b^2=6$, and $R(x,y)=\exp\{-x^2/c^2-y^2/d^2\}$, $c^2=6$, $d^2=28$; see Eq. 1]. The convolution is scaled by a factor of $[1+(c/a)^2][1+(d/b)^2]^{1/2}$ in order to compensate for the reduced refractive change due to the nonlocality.

The problem (see Eq. 1) of retrieving the spatial profile of the nonlocal response function $R(x,y)$ from the 2D refractive index distribution at a known intensity profile $I_p(x,y)$ of the laser beam is essentially an inverse problem, which could be solved by Fourier-deconvolution⁹. For real, non-negative and localized $I_p(x,y)$ and $R(x,y)$ the Fourier transforms $\mathcal{F}[I(x,y)]=I_p(k_x,k_y)$ and $\mathcal{F}[R(x,y)]=R(k_x,k_y)$ should exist. According to the Fourier convolution theorem $\mathcal{F}[\Delta n]=\mathcal{F}[R^*I_p]=\mathcal{F}[R]\mathcal{F}[I_p]=R(k_x,k_y)I_p(k_x,k_y)$, i.e. $R(k_x,k_y)=\mathcal{F}[R^*I_p]/I_p(k_x,k_y)$. Applying the inverse transformation

$$R(x,y)=\mathcal{F}^{-1}[R(k_x,k_y)]=\mathcal{F}^{-1}[\mathcal{F}[\Delta n]/I_p(k_x,k_y)], \tag{2}$$

one gets the response function $R(x,y)$. As seen from Eq. 1 and Eq. 2, the reconstruction procedure requires knowledge of the 2D refractive index distribution (Δn) inside the thermal medium. It can be obtained interferometrically¹⁸, which we

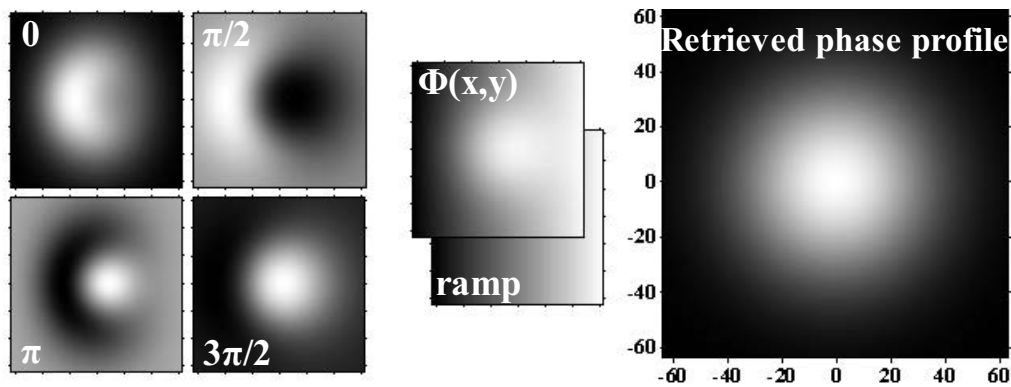


Fig. 2. Quantitative phase measurement: Set of four interference pictures at constant mutual phase offsets of $\pi/2$, reconstructed phase $\Phi(x,y)$, from which the phase ramp has to be subtracted in order to retrieve the phase profile of the probe beam.

illustrate in Fig. 2 in the particular realization of a four-frame technique. It relies on recording of a set of four interference patterns $I_j(x,y)$ ($j=1...4$) for given phase shifts of $0, \pi/2, \pi,$ and $3\pi/2$ between the object and the reference beams. Thereafter, the wavefront (phase profile) in the object arm of the interferometer can be reconstructed according to the relation $\Phi(x,y)=\tan^{-1}[(I_4-I_2)/(I_1-I_3)]$. Having found the phase distribution induced by the pump beam in the medium, the nonlocal response function can be determined from the deconvolution relation Eq. 2. However, direct application of this relation is not feasible as it leads to low accuracy in the regions of small signal. The most effective way is to employ iterative numerical scheme as described in Ref. [9].

3. EXPERIMENTAL PROCEDURE

In order to perform a pump-probe experiment in a thermal nonlinear medium, the wavelength of the light source inducing thermal effect has to be suitably absorbed by the sample. On the other hand the sample has to be transparent at the wavelength of the probe beam. In the experiment described here we used a 2 mm thick glass cell filled with Ethylene glycol dyed with Iodine. It absorbed 0.42% at 532 nm (pump wavelength) and less than 0.04% at 633 nm (probe wavelength). The experimental setup is shown in Fig. 3. The cell was placed in the object arm of an interferometer together with a programmable liquid-crystal phase modulator (PPM X8267, Hamamatsu) acting as an effective controllable mirror. After the modulator the first diffraction order beam was selected in a spatial filter and was used to introduce the desired phase shift of a multiple of $\pi/2$ in the object arm. The pump beam was injected in and ejected out of the object arm by a pair of polarizing beamsplitter cubes. The data acquisition was carried out with a 1024x1280 pix. charge-coupled device camera of 4 μm resolution (uEye 2240-M, IDS).

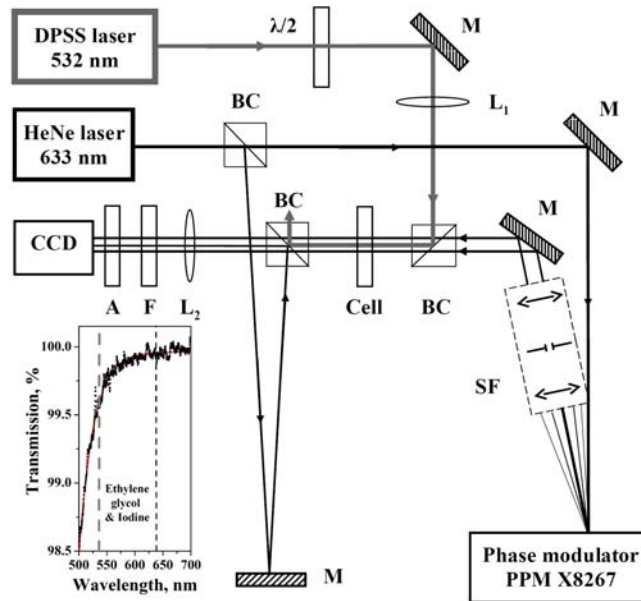


Fig. 3. Experimental scheme: DPSS laser, continuous-wave diode-pumped solid state laser with an intracavity second-harmonic generation ($\lambda=532$ nm); HeNe laser – Helium-Neon laser ($\lambda=633$ nm); $\lambda/2$, half wave plate; BC, polarizing beamsplitter cubes; SF, spatial filter; $L_{1,2}$, lenses of 250 mm and 80 mm focal lengths, respectively; M, silver-coated mirrors; F, red filter; A, analyzer; CCD, charge-coupled device camera. Inset: Dispersion of the transmission of the liquid sample with indicated pump and probe wavelengths (vertical dashed lines).

To maintain temporal stability of the interferometric measurements the experimental setup was built on a vibration-isolated table and enclosed in a flow-isolating box. The linear stability of the setup was checked by two successive retrievals of the linear phase front in the object arm. If the desired stability was achieved (mean phase difference between the two retrievals of, typically, less than 10^{-2} radians over the whole CCD-camera array), the pump beam was unblocked and passed through the sample. Ones again, two sets of four interferograms at controlled phase offsets and two successive retrievals of the nonlinear phase front were used to evaluate the stability during the measurement. If the predetermined stability criterion was met the data was smoothed out to remove high frequency noise and an array of 1024x1024 pixels was processed by using the Fourier-deconvolution iterative algorithm.

4. RESULTS AND DISCUSSION

In Fig. 4(a) we show the retrieved 2D nonlinear refractive index distribution $\Delta n(I(x,y))$ (see Eq. 1) representing the thermal lens created in the sample. Fig. 4(b) shows the energy-density profile of the pump laser both as a grayscale contour and surface plots. One can clearly recognize the significant difference between the fundamental Gaussian mode of the pump laser and the induced refractive-index distribution. Following the above-described procedure we

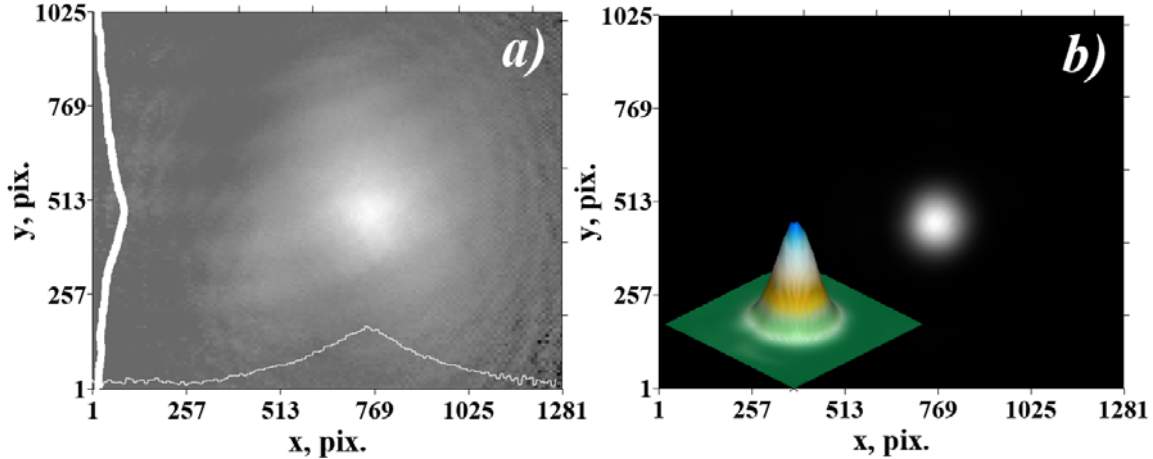


Fig. 4. (a) Retrieved refractive index distribution $\Delta n(I(x,y))$ and corresponding vertical and horizontal cross-sections; (b) Gaussian beam shape of the pump laser.

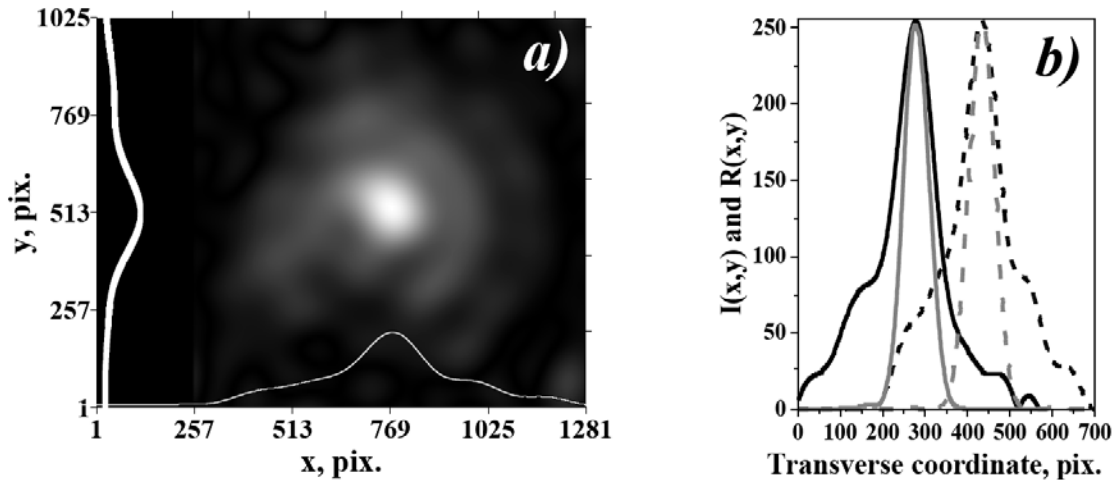


Fig. 5. (a) Reconstructed response function $R(x,y)$ of the thermal nonlinear medium; (b) Comparison of vertical (solid curves) and horizontal cross-sections (dashed) of $R(x,y)$ and $I(x,y)$ (black and gray, respectively) allowing to estimate the strength of the nonlocality.

reconstructed the nonlocal response function $R(x,y)$ of the thermal nonlinearity in Ethylene glycol. The experiment was repeated several times varying the input pump beam power (up to 6 mW, always below the threshold for appearance of convective flow in the liquid) and by focusing the pump beam at several different positions in the central part of the sample. In Fig. 5(a) we show the spatial profile of the retrieved nonlocal response function $R(x,y)$. The fact that the response is localized, real, and non-negative function is clearly seen and is in an agreement with the expectations^{10,15}. It is also evident that $R(x,y)$ consists of two qualitatively different components. The central peak, comparable in width with the laser beam itself, can be interpreted as the nonlocal response of an infinite sample. On the other hand, presence of broad wings is a characteristic feature of thermal effect. While the liquid is heated by the localized pump beam the heat conduction leads to a temperature increase in region located far away from the beam.

As a matter of fact, in a steady state, the thermal response of the medium is determined not only by the strength of the heat source but also by the boundaries of the medium. Therefore the long tails of the response function are directly related to the presence of the cell's boundaries. As Fig. 5 shows, the retrieved nonlocal response function is slightly distorted. The origin of this effect has nothing to do with thermal nonlinearity and is most likely caused by inhomogeneities of the probe beam. Our current efforts are directed towards rectifying this problem.

5. CONCLUSIONS

We have developed and demonstrated a novel experimental technique for retrieving the spatial profile of a long-range response function of a nonlocal nonlinear medium. We have shown that this method allows representing accurately the nonlocal response of a liquid with a nonlinearity of thermal origin. We believe that this method will be also useful for other nonlinear media including those with strong anisotropic nonlocal properties, and we are developing further alternative deconvolution procedures and comparative numerical simulations.

ACKNOWLEDGMENTS

This work was partially supported by the National Science Fund (Bulgaria), project F-1303/2003, and the Australian Research Council through the Discovery grant program.

REFERENCES

- 1.A. Litvak, V. Mironov, G. Fraiman, and A. Yunakovskii, *Sov. J. Plasma Phys.* 1, 31-37 (1975).
- 2.D. Suter and T. Blasberg, *Phys. Rev. A* 48, 4583-4587 (1993).
- 3.S. Gatz and J. Herrmann, *Opt. Lett.* 23, 1176-1178 (1998).
- 4.B. Crosignani, A. Degasperis, E. DelRe, P. Di Porto, and A. Agranat, *Phys. Rev. Lett.* 82, 1664-1167 (1999).
- 5.S. Akhmanov, D. Krindach, A. Migulin, A. Sukhorukov, and R. Khokhlov, *IEEE J. Quant. Electron.* 4, 568-575 (1968).
- 6.M. Iturbe-Castillo, J. Sanchez-Mondragon, and A. Stepanov, *Opt. Letters.* 21, 1622-1624 (1996).
- 7.C. Rotschild, O. Cohen, M. Segev, and T. Carmon, *Phys. Rev. Lett.* 95, 213904(1-4) (2005).
- 8.J. Wyller, *Physica D* 157, 90-111 (2000).
- 9.L. Gurdev, T. Dreischuh, and D. Stoyanov, *J. Opt. Soc. Am. A* 10, 2296-2306 (1993).
- 10.W. Krolikowski and O. Bang, *Phys. Rev. E* 63, 016610(1-6) (2000).
- 11.D. Briedis, D. Petersen, D. Edmundson, W. Krolikowski and O. Bang, *Optics Express* 13, 435-443 (2005).
- 12.A. Yakimenko, Yu. Zaliznyak, and Yu. Kivshar, *Phys. Rev. E* 71, 065603(R1-R4) (2005).
- 13.A. Dreischuh, D. N. Neshev, D. E. Petersen, O. Bang, and W. Krolikowski, *Phys. Rev. Lett.* 96, 043901(1-4) (2006).
- 14.Z. Xu, Y. V. Kartashov, and L. Torner, *Phys. Rev. Lett.* 95, 113901(1-4) (2005).
- 15.J. Wyller, W. Krolikowski, O. Bang, and J. Rasmussen, *Phys. Rev. E* 66, 066615(1-13) (2002).
- 16.A. Snyder and J. Mitchell, *Science* 276, 1538-1541 (1997).
- 17.D. J. Mitchell and A. W. Snyder, *J. Opt. Soc. Am. B* 16, 236-239 (1999).
- 18.C. Creath, *Holographic Interferometry*, Springer, Berlin, 1994; Th. Kreis, *Holographic Interferometry: Principles and Methods*, Akademie-Verlag, Berlin, 1996.